JOURNAL OF SOLID STATE CHEMISTRY 119, 412–419 (1995)

A New Layered Structure Based on Perovskite in the $SrO–La_2O_3–TiO_2$ System

M. E. Bowden,*[,1] D. A. Jefferson,* and I. W. M. Brown†

*Department of Chemistry, University of Cambridge, Lensfield Road, Cambridge CB2 1EW United Kingdom; and †New Zealand Institute for Industrial Research and Development, P.O. Box 31-310, Lower Hutt, New Zealand

Received December 30, 1994; in revised form June 14, 1995; accepted June 15, 1995

A new compound, $Sr_3La_2Ti_2O_{10}$, has been prepared and characterized by a combination of X-ray diffraction and high-resolution electron microscopy. It is monoclinic (space group $P2_1/m$, $a = 6.9159(3)$ Å, $b = 5.5252(2)$ Å, $c = 12.2953(7)$ Å, and $\beta = 85.443(4)°$) and refinement of metal positions has been carried out using Rietveld analysis. The structure contains corner-sharing TiO_6 octahedra like those in perovskite, but arranged in ribbons separated by rock-salt layers of Sr/La atoms. The ribbons are one octahedron high and four octahedra wide; efforts to prepare compounds with different widths resulted in mixed layer intergrowths. This new structure may be part of a wider family containing essentially one-dimensional elements of perovskite of special interest to high-temperature superconductivity.

INTRODUCTION

Interest in compounds possessing a layered structure based on perovskite has intensified in recent years following the discovery of the high-temperature superconducting oxides. We described recently (1) how oxygen-rich layers parallel to {110} are introduced into the perovskite $SrTiO_3$ by substituting La^{3+} for Sr^{2+}. Following this study, we investigated the possibility of La substitution in the so-called "Ruddlesden–Popper" compounds $Sr_{n+1}Ti_nO_{3n+1}$ (2, 3). These compounds contain double layers of Sr atoms parallel to perovskite {100} planes, interleaved with blocks of perovskite n octahedra wide. Our interest in this investigation was to see whether the substitution would result in a combination of {100}- and {110}-type layers. The experiments produced unidentifiable peaks in X-ray diffraction patterns, suggesting the formation of a hitherto uncharacterized compound. This report describes the identification and structure of this new phase, based on high-resolution electron microscope images and Rietveld analysis of X-ray diffraction patterns.

[1] Current address: New Zealand Institute for Industrial Research and Development, P.O. Box 31-310, Lower Hutt, New Zealand.

EXPERIMENTAL

Specimens were prepared by conventional solid-state synthesis using $SrCO_3$, La_2O_3, and TiO_2 as starting materials. Because of the hydroscopic nature of La_2O_3, a stock of La_2TiO_5 was prepared to use as a source of La by drying La_2O_3 at 800°C and immediately weighing it before blending and firing with TiO_2. Weighed mixtures of $SrCO_3$, La_2TiO_5, and TiO_2 were ground together and fired overnight in air at 1350°C. The process of grinding and firing was repeated until no significant change could be seen in the X-ray diffraction patterns.

X-ray diffraction (XRD) patterns were collected using a computer-controlled Philips goniometer and Cu$K\alpha$ radiation. Patterns for Rietveld analysis were collected as step scans, counting for 4 sec at 0.04° 2θ intervals. These conditions were chosen according to the recommendations of Hill and Madsen (4), using a step size approximately $\frac{1}{3}$ the peak width and giving a maximum intensity slightly larger than the 10,000 counts recommended. Structural refinement from these patterns was carried out using RIET7, an extensively modified version of the DBWS program described by Wiles and Young (5). The parameters refined are summarized in Table 1.

Samples for examination by high-resolution electron microscopy (HREM) were prepared by dispersing a suspension of the powder in acetone over holey carbon film. A JEOL 200CX instrument fitted with a high-resolution (C_s = 0.41 mm) pole piece was operated at 200 kV and magnifications ≈500,000×. Simulated images were calculated by the multi-slice method with the commercially available CERIUS software (Molecular Simulations Inc.). Values describing the microscope properties were the same as those established for successful simulation of known compounds used in previous studies (1).

RESULTS AND DISCUSSION

1. Formulation of a Draft Structure

In order to establish the composition of the unidentified phase, a range of compositions was prepared and examined

0022-4596/95 $12.00

TABLE 1
Summary of Parameters Refined during Rietveld Analysis

Description	Number of parameters
Diffractometer zero	1
Profile shape factors (psuedo-Voigt)	3
Profile width factors	3
Profile asymmetry	1
Background (polynomial series)	4
Scale factor	1
Lattice parameters	4
Atomic coordinates	16
Sr/La site occupancy	1
Isotropic temperature factors	3

by XRD. The intensities of the unidentified peaks reached a maximum at a composition corresponding to the formula $Sr_3La_2Ti_2O_{10}$, and peaks from known compounds could no longer be detected.

Electron diffraction patterns taken from this sample suggested a monoclinic cell with the approximate dimensions a = 6.9 Å, b = 5.5 Å, c = 12.2 Å, and β = 85°. HREM images taken in the [010] direction (see Fig. 4 below) clearly showed that the compound possessed a layered structure. Within each layer, rows of dots could be discerned spaced at ≈2.8 Å intervals and inclined at ≈70° to the plane of the layers. The perpendicular separation between the rows of dots was ≈6.3 Å.

The spacing of 2.8 Å is consistent with a perovskite-based structure since this is the width of the TiO_6 octahedra found in $SrTiO_3$. Although the spacing of 6.3 Å is not encountered in perovskite, it can be recognized as the distance between layers in the Ruddlesden–Popper compound Sr_2TiO_4.

From all of these considerations a structure was proposed (Fig. 1a) consisting of ribbons of TiO_6 octahedra one octahedron high and four octahedra wide extending along the b axis. The configuration of these ribbons and intervening Sr/La atoms resembles blocks of the Sr_2TiO_4 structure cut along (112) planes. To highlight this, a view of the Sr_2TiO_4 structure is also shown in Fig. 1b. The blocks are layered above one another and additional Sr/La atoms are positioned in the interlayer spaces that are created. Preliminary HREM image simulations showed good agreement with the observed micrographs, and so this structure was used for input to the Rietveld refinement program.

2. *Rietveld Refinement*

The dimensions of the unit cell led to many potential diffraction peaks spaced closely together, which made the assignment of a space group based on systematic absences difficult. Instead, a space group was chosen from the monoclinic groups which possessed the symmetry elements of the proposed structure, beginning with the most symmetric. This was input to the Rietveld procedure, followed by less symmetric groups until the reduction in symmetry did not account for further peaks in the observed diffraction pattern. Using this procedure, space group $P2_1/m$ was selected.

With all the atomic parameters unconstrained, the refinement converged to give a good agreement between observed and calculated diffraction patterns, although two structural considerations made the result questionable. First, the refinement gave an unreasonably wide variation of oxygen temperature factors, with large standard deviations. To avoid this, a single thermal parameter was refined for all the oxygens in the structure. The second problem was that the positions of oxygen atoms around TiO_6 octahedra resulted in considerable distortion where there seemed no structural reason why this should be so. For example, oxygens linking adjacent TiO_6 octahedra were placed much closer to one of the titanium atoms than the other. For the final refinement, the positions of oxygen atoms forming TiO_6 octahedra were adjusted to give little distortion and to maintain bond lengths close to the expected distance of 2.0 Å. The fit with these oxygen positions constrained was only slightly poorer, with the agreement index R_{wp} equal to 9.1% as opposed to 9.0% for the unconstrained refinement. The difficulty in defining oxygen positions and temperature factors was considered to be due to the relative insensitivity of the calculated XRD pattern to these parameters. Similarly, the temperature factors for the metal atoms were refined in groups to avoid occasional negative values.

Partitioning of strontium and lanthanum over the available sites was not able to be determined completely because the refinement program did not allow the partial occupancy of these elements to be refined while main-

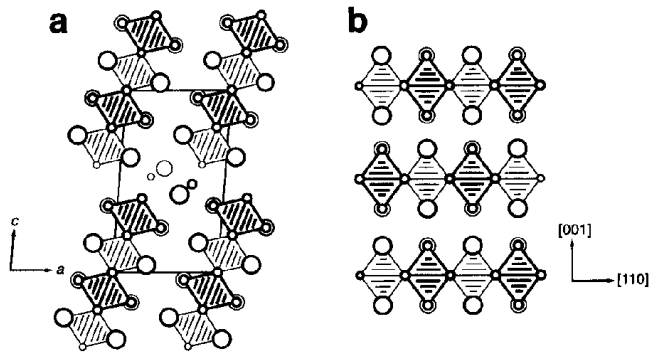

FIG. 1. Structural diagrams of (a) the proposed $Sr_3La_2Ti_2O_{10}$ structure and (b) Sr_2TiO_4. Ti atoms lie at the centers of the octahedra, small circles represent O atoms, and large circles represent Sr/La atoms. Heavy ruling indicates a difference in height of $b/2$ perpendicular to the plane of projection.

TABLE 2
Final Refined Coordinates

Atom	Site	x	y	z	Occ. (Sr)	B (iso)
Ti(1)	2e	0.060(4)	¾	0.1036(19)		0.2(3)
Ti(2)	2e	0.174(4)	¼	0.3171(19)		0.2(3)
Sr/La(1)	2e	0.3161(25)	¼	0.0517(11)	0.84(2)	0.20(11)
Sr/La(2)	2e	0.4371(17)	¾	0.2498(11)	0.442(14)	0.20(11)
Sr/La(3)	2e	−0.1833(24)	¼	0.1558(10)	0.84(2)	0.20(11)
Sr/La(4)	2e	−0.0473(20)	¾	0.3915(11)	0.442(14)	0.20(11)
Sr/La(5)	2e	0.4113(15)	¾	0.5624(9)	0.442(14)	0.20(11)
O(1)	2a	0	0	0		1.7(3)
O(2)	4f	0.119	0	0.207		1.7(3)
O(3)	4f	0.268	0	0.416		1.7(3)
O(4)	2e	0.343	¾	0.055		1.7(3)
O(5)	2e	0.433	¼	0.231		1.7(3)
O(6)	2e	−0.223	¾	0.153		1.7(3)
O(7)	2e	−0.084	¼	0.403		1.7(3)
O(8)	2e	0.368(11)	¼	0.628(6)		1.7(3)

Note. Figures in parentheses indicate the estimated standard deviation of the last significant figures. The refined lattice parameters were a = 6.9214(4) Å, b = 5.5294(3) Å, c = 12.3048(8) Å, and β = 85.439(4)°, and the Bragg R factor was 4.17%.

taining a constant overall stoichiometry. When the occupancies were relaxed, a strong tendency for Sr to concentrate in sites near the center of the Sr_2TiO_4 blocks (Sr/La(1) and (3), Table 2) was observed. Lanthanum occupancy was highest in the site between the Sr_2TiO_4 blocks (Sr/La(5)). However, since only one occupation parameter could be refined without altering the total amounts of these elements, Sr and La were distributed between sites 1 and 3, and sites 2, 4, and 5 for the final refinement.

Figure 2 compares the observed and calculated diffraction patterns, and the refined structural parameters are presented in Table 2. The small peaks in the difference pattern evident near 30°, 46°, 52°, and 58° indicate the presence of an unidentified second phase and were excluded from the Rietveld refinement. The indexed XRD pattern is listed in Table 3.

The refined titanium positions led to a slight buckling of the Ti–O ribbons rather than the linear arrangement shown in the idealized view of Fig. 1a. The Sr/La sites within the Sr_2TiO_4 blocks have the same nine-fold coordination as found in Sr_2TiO_4 itself, except for Sr/La(4) which has two additional oxygen neighbors from the adjacent Sr_2TiO_4 block. Since most of the structure is derived directly from Sr_2TiO_4, the key as to whether it is structurally sensible lies with the additional site placed between the Sr_2TiO_4 blocks. A stereoscopic view of the coordination

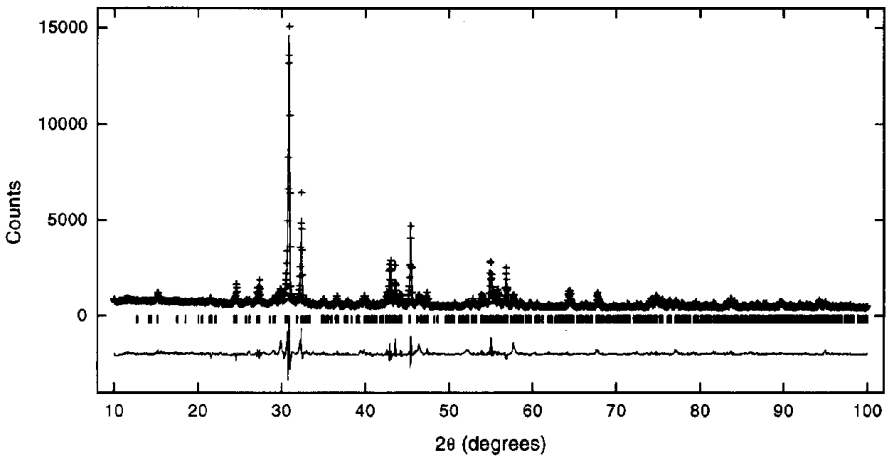

FIG. 2. Observed (dots), calculated (line), and difference (lower) plots of the X-ray diffraction pattern of $Sr_3La_2Ti_2O_{10}$. The markers indicate the positions of all allowed reflections.

TABLE 3
X-Ray Diffraction Peaks for $Sr_3La_2Ti_2O_{10}$

h	k	l	d(calc)	d(obs)	I/I_0	h	k	l	d(calc)	d(obs)	I/I_0
1	0	−1	5.815	5.816	3	4	0	−3	1.5446	1.5450	1
1	1	1	4.132	4.131	2	3	1	6	1.5287	1.5297	1
0	1	2	4.104	4.099	1	2	2	−6	1.4473	1.4479	5
1	0	3	3.644	3.641	2	4	2	2	1.4445	1.4442	6
1	1	2	3.612	3.611	7	2	0	8	1.4432		
2	0	0	3.447	3.448	1	4	1	5	1.4167	1.4168	1
1	0	−3	3.398	3.401	2	4	2	−2	1.4012	1.4003	1
0	1	3	3.285	3.283	6	0	4	0	1.3813	1.3816	5
2	0	−1	3.252	3.250	9	4	2	−3	1.3482	1.3486	1
0	0	4	3.064	3.068	2	4	1	−5	1.3206	1.3208	1
1	1	3	3.042	3.040	3	2	0	9	1.3024	1.3032	1
1	1	−3	2.895	2.895	68	2	3	6	1.2953	1.2957	1
2	1	1	2.889	2.888	100	1	1	−9	1.2804	1.2804	2
1	0	4	2.886			3	3	−4	1.2770	1.2770	3
0	2	0	2.763	2.762	41	0	3	7	1.2690	1.2689	4
2	1	2	2.711	2.711	2	5	1	4	1.2622	1.2628	2
1	2	0	2.564	2.562	2	4	3	0	1.2584	1.2589	3
0	0	5	2.451	2.452	3	1	4	4	1.2460	1.2467	3
2	0	4	2.386	2.386	1	4	1	−6	1.2364	1.2368	3
1	0	5	2.370	2.371	2	5	2	2	1.2264	1.2268	2
1	2	−2	2.341	2.340	1	3	2	−7	1.2073	1.2076	1
1	0	−5	2.254	2.256	4	3	3	6	1.2039	1.2044	2
1	2	3	2.201	2.200	1	2	1	−9	1.2039		
3	1	0	2.122	2.122	4	1	0	−10	1.1905	1.1910	1
3	1	1	2.117	2.116	4	2	2	9	1.1781	1.1785	2
2	2	−1	2.105	2.105	14	4	2	7	1.1615	1.1619	1
3	0	−2	2.098	2.099	16	5	2	−3	1.1584	1.1588	2
3	0	3	2.075	2.075	15	3	4	−2	1.1536	1.1540	3
2	1	−4	2.048	2.047	4	3	4	3	1.1498	1.1504	2
0	0	6	2.043	2.043	3	5	1	−5	1.1380	1.1385	1
1	2	4	1.9958	1.9959	28	5	0	7	1.1277	1.1281	1
1	0	−6	1.9175	1.9175	5	1	4	−6	1.1208	1.1208	1
1	2	5	1.7987	1.7999	1	6	1	−1	1.1124	1.1127	1
2	1	6	1.7303	1.7315	2	3	1	−9	1.1097	1.1101	1
2	0	−6	1.6991	1.6999	4	1	2	−10	1.0933	1.0938	2
3	1	−4	1.6874	1.6884	2	1	1	11	1.0920	1.0923	2
3	2	−2	1.6706	1.6701	16	6	1	−2	1.0915		
0	1	7	1.6691			5	1	−6	1.0816	1.0822	1
3	2	3	1.6589	1.6595	5	2	4	−6	1.0718	1.0714	1
4	1	0	1.6453	1.6455	6	6	2	1	1.0637	1.0642	1
1	3	−3	1.6192	1.6195	14	5	3	4	1.0602	1.0605	1
2	3	1	1.6182			1	5	−3	1.0509	1.0511	3
1	2	−6	1.5752	1.5756	2	5	2	7	1.0440	1.0446	2
2	1	7	1.5490	1.5492	1	4	1	10	1.0207	1.0211	1

around this site is presented in Fig. 3 which shows it to be 9-coordinated with its oxygen atoms reasonably distributed around the central metal atom. The metal–oxygen distances are in the range 2.17–2.94 Å, comparable to the other Sr/La atoms.

3. *High-Resolution Electron Microscopy*

Further confirmation of the proposed structure was sought by comparing simulated and observed HREM images. The agreement was good, as shown in Figs. 4 and 5 for images taken in the [010] and [100] directions, respectively. A notable feature of the [100] images was the dramatic change in contrast with increasing distance from the crystal edge, presumably due to increasing crystal thickness. The image simulations reproduced this behavior well. Near the crystal edge the simulation matches the observed image in general appearance, but exhibits a greater level of detail than the micrograph (Fig. 5b). In fact, most of the images recorded from this compound showed poorly ordered or amorphous regions near the edge, and it was thought that some degree of surface disorder was always present.

Further from the edge, the micrograph contained a region of confused detail but with strong diagonal fringes, also contained in the simulated image (Fig. 5c) for 145-Å thick crystals. It was only at comparatively large crystal thicknesses that the micrograph displayed a clear and regular pattern. The simulated images (Figs. 5d and 5e) provided the best match in these regions. It should be noted that although this micrograph exhibited the greatest detail of those recorded in the [100] direction, a consistent beam tilt of 2 mrad around b needed to be incorporated into image simulations to achieve satisfactory comparisons. Nevertheless, the fact that good agreement was obtained over a large range of thicknesses with sensible defocus values strongly suggests that the cation positions in the proposed structure are correct.

Most of the HREM images obtained from the $Sr_3La_2Ti_2O_{10}$ sample were, apart from surface disorder, relatively free of defects. A notable exception to this observation is shown in Fig. 6 which shows a coherent boundary between $Sr_3La_2Ti_2O_{10}$ on the right and a region with a different structure containing irregular faults on the left. Direct measurement of the lattice combined with image simulations confirmed that this was a region of perovskite structure, viewed in the [110] direction. The arrangement of octahedra in $Sr_3La_2Ti_2O_{10}$ is such that a transition to the perovskite structure can be achieved without undue strain. Figure 7 illustrates how this is accomplished through the registration of perovskite octahedra with those in the ribbons in $Sr_3La_2Ti_2O_{10}$. The linear faults visible within

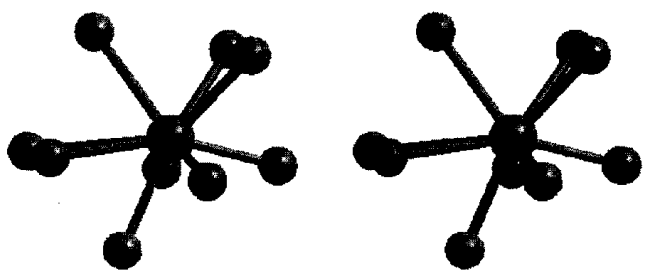

FIG. 3. Stereographic projection of the oxygen coordination around Sr/La(5), viewed slightly off the b direction.

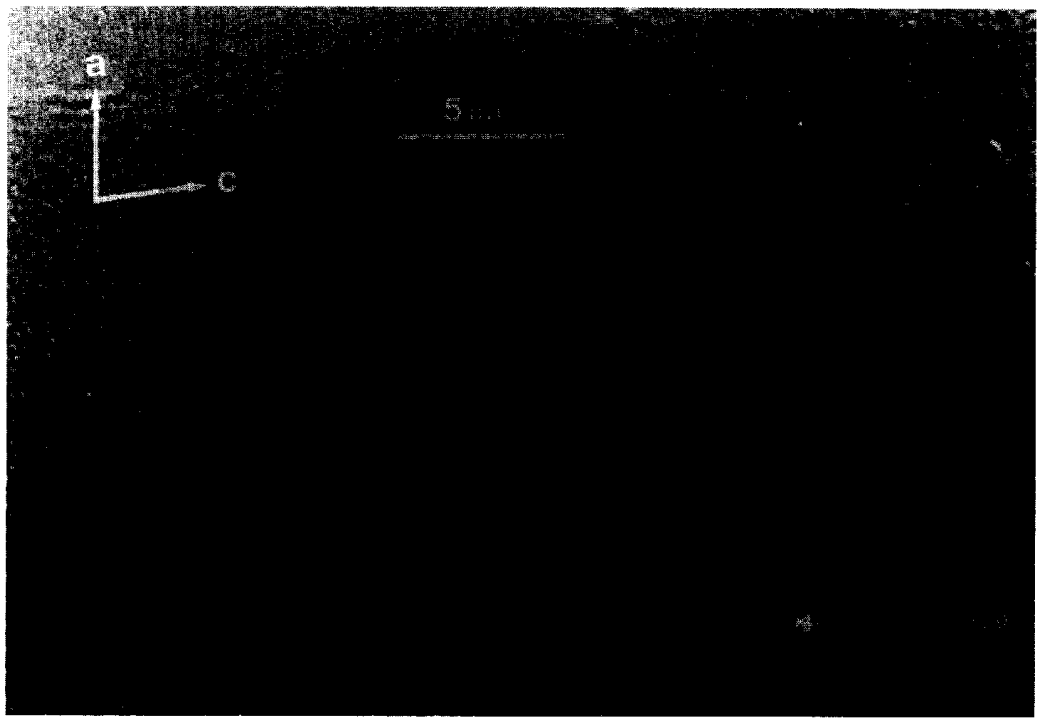

FIG. 4. [010] HREM image and electron diffraction pattern with simulated image inset for a 33-Å thick crystal at a defocus of −225 Å.

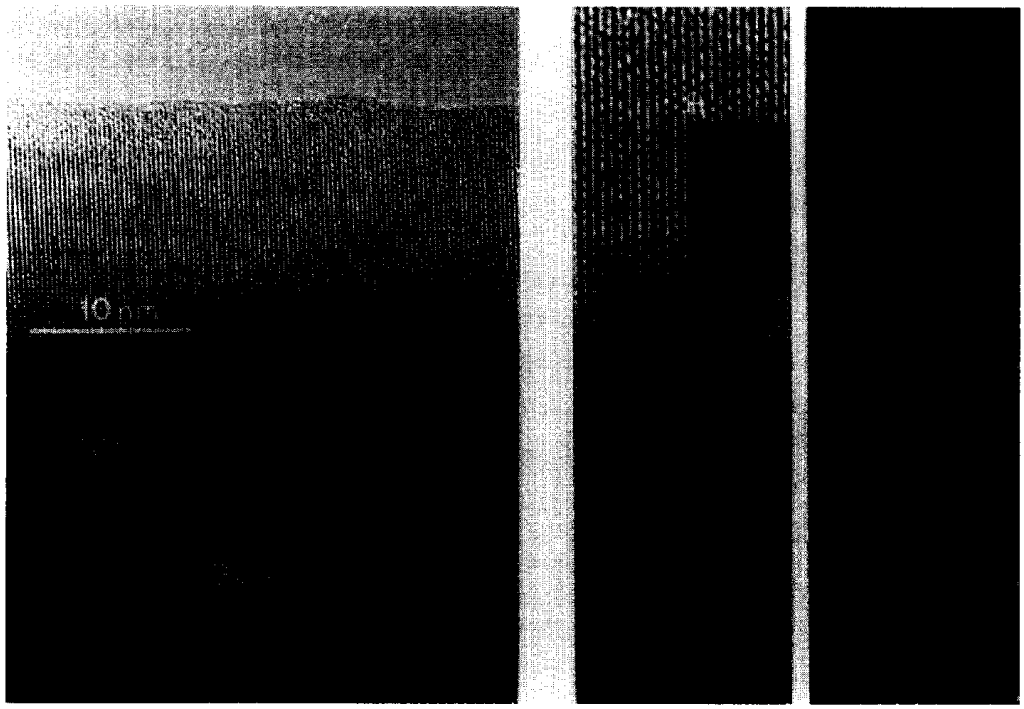

FIG. 5. (A) [100] HREM image and electron diffraction pattern. The enlarged section on the right includes simulated images for (B) thickness = 35 Å, defocus = −275 Å; (C) thickness = 145 Å, defocus = −325 Å; (D) thickness = 221 Å, defocus = −400 Å; and (E) thickness = 242 Å, defocus = −425 Å. A beam tilt of 2 mrad around *b* is included in all simulations.

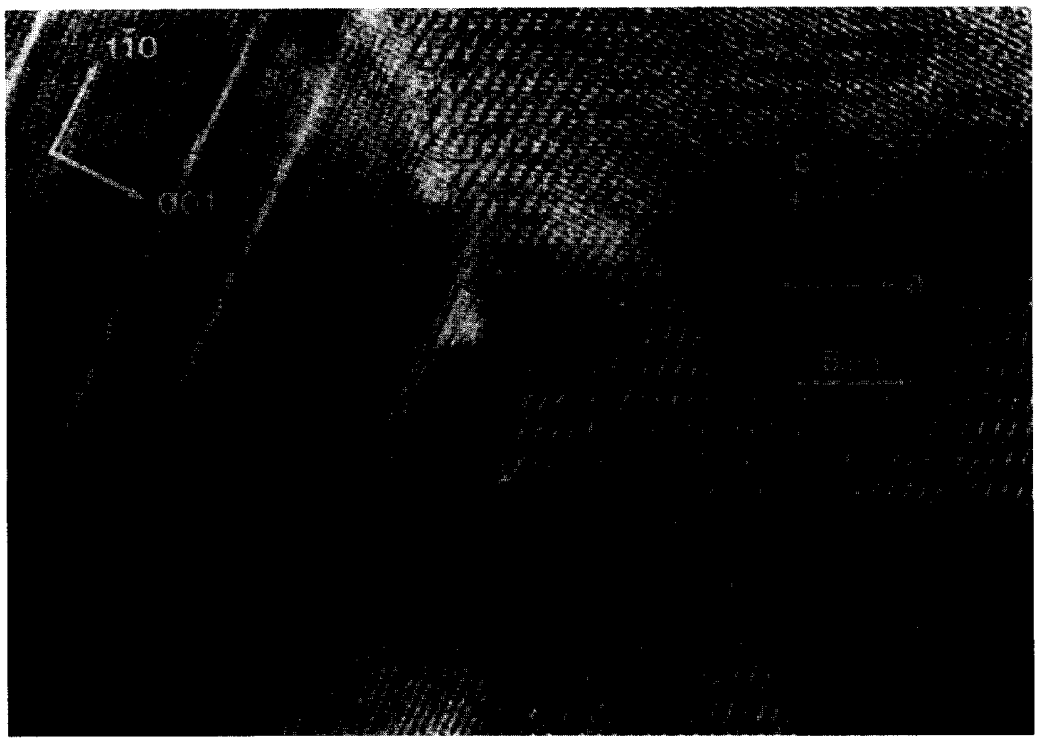

FIG. 6. Disordered crystal fragment showing interface between $Sr_3La_2Ti_2O_{10}$ on the right and faulted perovskite on the left. The electron diffraction pattern of $Sr_3La_2Ti_2O_{10}$ can be indexed by analogy with Fig. 4.

the perovskite region in Fig. 6 can be identified as layers of the rock-salt structure, as found in the Ruddlesden–Popper compounds (2, 3). Their appearance and uneven spacing strongly resemble those observed by Fujimoto *et al.* in their study of the alkaline earth excess perovskite $(Sr_{0.85}Ca_{0.15}O)_{1.02} \cdot TiO_2$ (6).

Because of its layered structure, $Sr_3La_2Ti_2O_{10}$ presents the potential for a family of related compounds containing different layer thicknesses. $Sr_3La_2Ti_2O_{10}$ has two layer types; therefore related materials might be generated either by varying the parent Ruddlesden–Popper compound that forms each block or by altering the block width. The first of these possibilities was considered unlikely since registration of overlying blocks does not occur with structures comprising Ruddlesden–Popper compounds other than Sr_2TiO_4. On the other hand, compounds containing Sr_2TiO_4 blocks of different widths appear structurally feasible and lead to a family with the general formula $Sr_{2n-2}La_4Ti_nO_{4n+4}$. In this formula, n represents the number of TiO_6 octahedra across the width of the Sr_2TiO_4 block, making $Sr_3La_2Ti_2O_{10}$ the $n = 4$ member.

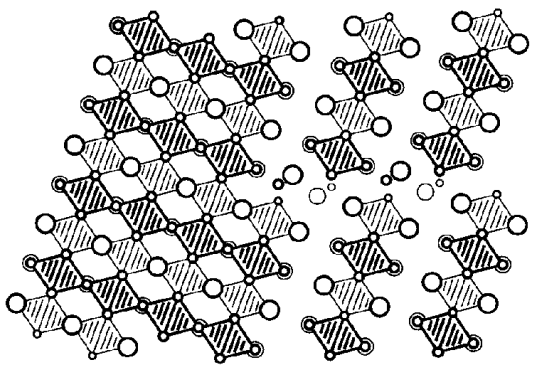

FIG. 7. Structural diagram illustrating a coherent boundary between $Sr_3La_2Ti_2O_{10}$ and perovskite, as observed in the micrograph shown in Fig. 6.

Samples with values of n ranging from 3 to 7 were reacted in an effort to prepare other members of the $Sr_{2n-2}La_4Ti_nO_{4n+4}$ family. No ordered compounds beside $Sr_3La_2Ti_2O_{10}$ could be detected by either HREM or XRD. For the $n = 3$ composition XRD showed the sample to contain $Sr_3La_2Ti_2O_{10}$ and La_2O_3, while broadened $Sr_3La_2Ti_2O_{10}$ peaks and minor amounts of Ruddlesden–Popper compounds were observed for compositions between $n = 5$ and 7. Disordered intergrowths of varying layer thicknesses were however observed in HREM images of higher n specimens. An example is shown in Fig. 8, recorded from a sample close to the $n = 5$ composition. For the most part, this area contains layers of the $n = 6$ structure seen in the [110] orientation, but layers with different widths are also clearly visible. Atomic coordinates for the $n = 6$ structure were calculated based on $Sr_3La_2Ti_2O_{10}$ and used for the

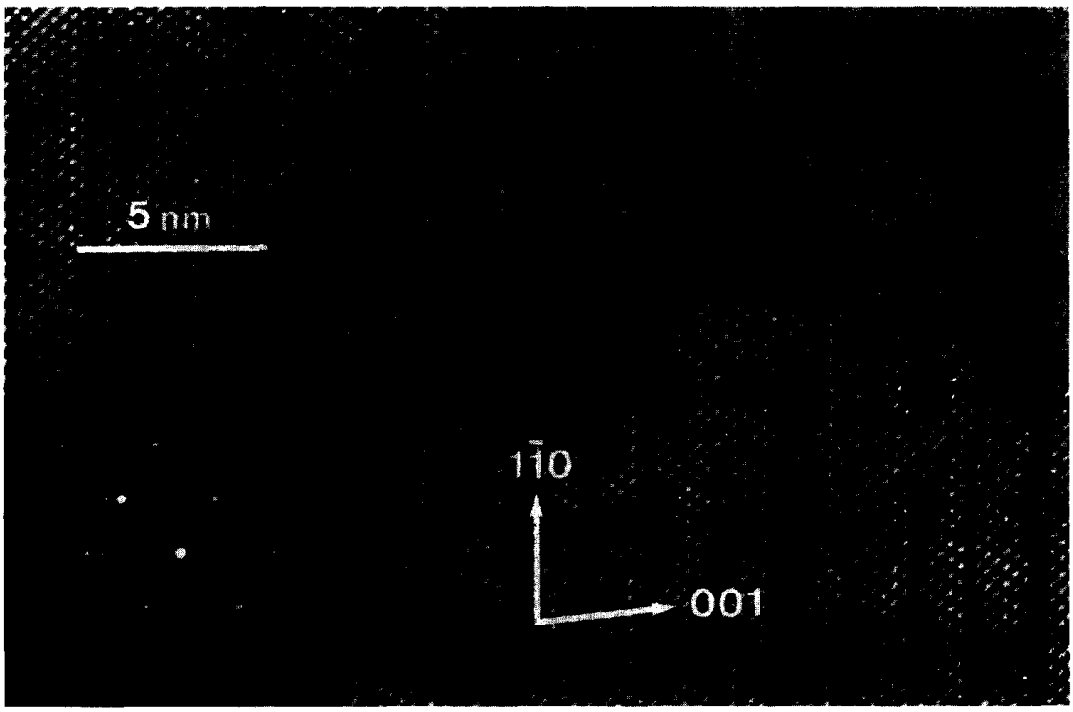

FIG. 8. [110] HREM image showing irregular intergrowth of $Sr_{2n-2}La_4Ti_nO_{4n+4}$ layers. The simulated image inset is for an $n = 6$ member 53-Å thick and at a defocus of −600 Å.

simulated image inset in Fig. 8. Although this particular region contains predominantly $n = 6$ layers, the electron diffraction pattern indicated a different layer spacing. Disorder in layer stacking was evident from the streaking of spots along the direction of c^*, but the discernible spots suggested a principle average distance of 14.9 Å between layers, which is the separation expected for the $n = 5$ compound. This discrepancy can be reconciled by noting that the diffraction aperture used covers a considerably larger area (≈6500 Å diameter) than that displayed in the micrograph. Hence it appears that while the average structure of this fragment may approximate that expected for $n = 5$, the microscopic detail shows that considerable local variation in layer thickness exists.

SUMMARY AND CONCLUSIONS

A new compound with the formula $Sr_3La_2Ti_2O_{10}$ has been identified in the SrO–La_2O_3–TiO_2 system. This compound can be envisaged as comprising blocks of the Sr_2TiO_4 structure (K_2NiF_4-type) formed by slicing Sr_2TiO_4 parallel to the (112) planes. The blocks are four octahedra wide and are stacked above one another with additional Sr/La atoms placed in the interstices created. To our knowledge, this is the first reported compound which possesses this structural arrangement.

Rietveld analysis was used to refine the positions of metal atoms but oxygen atoms were constrained in chemically sensible positions. Nevertheless, the proposed structure was considered to be essentially correct because of the corroborating evidence provided by high-resolution electron microscopy. This was indicated first by the close agreement between calculated and experimental images over a wide range of conditions. In addition, the manner in which the $Sr_3La_2Ti_2O_{10}$ structure was observed to mesh with that of perovskite verified the arrangement of oxygens in corner-sharing octahedra.

Although no similar compounds with different, regularly spaced layers could be prepared, the observation of disordered regions with mixed layer spacing suggested that $Sr_3La_2Ti_2O_{10}$ could be part of a general structural group of the type $A_{2n-6}B_nO_{4n+4}$. Such structures are relevant to the study of high-temperature superconductivity since they contain ribbons of corner-sharing octahedra which extend significantly in one dimension only. The transition from a three-dimensional to a two-dimensional arrangement is thought to be important for the onset of high-temperature superconductivity, and so the further reduction in dimensionality given by the $Sr_3La_2Ti_2O_{10}$ structure is of considerable interest.

ACKNOWLEDGMENT

M.E.B. gratefully acknowledges the financial assistance provided by the New Zealand Institute for Industrial Research and Development in carrying out this work.

REFERENCES

1. M. E. Bowden, D. A. Jefferson, and I. W. M. Brown, *J. Solid State Chem.* **117,** 88 (1995).
2. S. N. Ruddlesden and P. Popper, *Acta Crystallogr.* **10,** 538 (1957).
3. S. N. Ruddlesden and P. Popper, *Acta Crystallogr.* **11,** 54 (1958).
4. R. J. Hill and I. C. Madsen, *Powder Diffr.* **2,** 146 (1987).
5. D. B. Wiles and R. A. Young, *J. Appl. Crystallogr.* **14,** 149 (1981).
6. M. Fujimoto, J. Tanaka, and S. Shirasahi, *Jpn. J. Appl. Phys.* **27,** 1162 (1988).